HHS Public Access

Author manuscript

Brain Res. Author manuscript; available in PMC 2018 November 15.

Published in final edited form as:

Brain Res. 2017 November 15; 1675: 28–40. doi:10.1016/j.brainres.2017.08.031.

Neurochemical differences between target-specific populations of rat dorsal raphe projection neurons

Eric W. Prouty[a], **Daniel J. Chandler**[a,1], and **Barry D. Waterhouse**[a,1]

[a]Department of Neurobiology and Anatomy, Drexel University College of Medicine, Philadelphia PA 19129, USA

Abstract

Serotonin (5-HT)-containing neurons in the dorsal raphe (DR) nucleus project throughout the forebrain and are implicated in many physiological processes and neuropsychiatric disorders. Diversity among these neurons has been characterized in terms of their neurochemistry and anatomical organization, but a clear sense of whether these attributes align with specific brain functions or terminal fields is lacking. DR 5-HT neurons can co-express additional neuroactive substances, increasing the potential for individualized regulation of target circuits. The goal of this study was to link DR neurons to a specific functional role by characterizing cells according to both their neurotransmitter expression and efferent connectivity; specifically, cells projecting to the medial prefrontal cortex (mPFC), a region implicated in cognition, emotion, and responses to stress. Following retrograde tracer injection, brainstem sections from Sprague-Dawley rats were immunohistochemically stained for markers of serotonin, glutamate, GABA, and nitric oxide (NO). 98% of the mPFC-projecting serotonergic neurons co-expressed the marker for glutamate, while the markers for NO and GABA were observed in 60% and less than 1% of those neurons, respectively. To identify potential target-specific differences in co-transmitter expression, we also characterized DR neurons projecting to a visual sensory structure, the lateral geniculate nucleus (LGN). The proportion of serotonergic neurons co-expressing NO was greater amongst cells targeting the mPFC vs LGN (60% vs 22%). The established role of 5-HT in affective disorders and the emerging role of NO in stress signaling suggest that the impact of 5-HT/NO co-localization in DR neurons that regulate mPFC circuit function may be clinically relevant.

1. Introduction

Located at the midbrain-pontine border, the dorsal raphe (DR) nucleus contains the greatest number of serotonin (5-HT)-producing neurons in the central nervous system of both rodents and humans and is the major source of 5-HT to the mammalian forebrain (Baker et al., 1991;

Corresponding author: Barry D. Waterhouse, Department of Cell Biology and Neuroscience, Rowan University School of Osteopathic Medicine, Stratford, NJ 08084, USA; waterhouse@rowan.edu.

[1]Present address: Department of Cell Biology and Neuroscience, Rowan University School of Osteopathic Medicine, Stratford, NJ 08084, USA

The authors declare no conflicts of interest.

Vertes and Crane, 1997). Mounting evidence suggests there is an intrinsic organization within the DR that allows subsets of serotonergic neurons to regulate discrete physiological functions and behavioral outcomes (Commons, 2015; Gaspar and Lillesaar, 2012; Niederkofler et al., 2016). The possibility of such functional units is founded upon the now well-recognized diversity in the molecular profile, connectivity, electrophysiology, and neurochemistry of DR 5-HT neurons (Calizo et al., 2011; Fernandez et al., 2016; Hale and Lowry, 2011). DR 5-HT neurons can co-express additional neuroactive substances including several neuropeptides, the classic transmitters glutamate and γ-aminobutyric acid (GABA), and nitric oxide (NO) (Fu et al., 2010; Gaspar and Lillesaar, 2012). The expression of different neurotransmitter combinations may allow DR neurons to achieve differential modes of output and individualized regulation of specific target circuits. Therefore, an important question is whether brain regions with discrete functions are innervated by subsets of DR neurons with unique neurochemical profiles. The overarching goal of the present work was to link the neurochemical profile of DR projection neurons with specific efferent target circuit functions. We used retrograde tract tracing and immunofluorescence to examine the expression of serotonin and several putative co-transmitters (glutamate, GABA, and NO) in populations of DR neurons projecting to two functionally distinct brain regions —medial prefrontal cortex (mPFC) and the lateral geniculate nucleus (LGN) of the thalamus.

Originally delineated by Dahlström and Fuxe using vaporized formaldehyde, serotonergic neurons in the brainstem are now commonly identified using antibodies targeting serotonin itself or tryptophan hydroxylase (TPH), the rate-limiting enzyme of serotonin synthesis (Dahlström and Fuxe, 1964; Fu et al., 2010; Walther et al., 2003). The 5-HT-containing neurons of the DR are located between the cerebral aqueduct and the fiber tracts of the medial longitudinal fasciculus (MLF) at the level of the midbrain-pontine border (Hale and Lowry, 2011; Jacobs and Azmitia, 1992). When viewed in the coronal plane, natural anatomical subdivisions within the DR are formed by the clustering of these 5-HT-positive cells (Hale and Lowry, 2011; Paxinos and Watson, 1997); in this work, we will refer to three major subdivisions— dorsomedial, ventromedial and lateral (also called the lateral wings, LW).

Vesicular glutamate transporters (VGLUTs) are commonly used as neurochemical markers for glutamatergic neurons (Fremeau et al., 2004). All three VGLUT isoforms (VGLUT1-3) are present in the DR, though they differ in their patterns of distribution and subcellular localization (Commons et al., 2005; Gras et al., 2002). VGLUT1 and VGLUT2 are only observed in the presynaptic terminals of afferent inputs to DR, while only VGLUT3 is found within the cell bodies of DR neurons (Commons et al., 2005; Commons, 2009; Hioki et al., 2010). The unique localization of the VGLUT3 isoform within cell bodies makes it an ideal neurochemical marker for co-localization studies to identify serotonergic projection neurons that may be capable of releasing glutamate. The co-release of 5-HT and glutamate would have major implications for activity-dependent plasticity in target circuits and recent evidence suggests that VGLUT3 itself may influence 5-HT transmission by enhancing vesicular packing of 5-HT (Amilhon et al., 2010) or regulating the number of synaptic specializations formed by serotonergic axons (Gagnon and Parent, 2014; Voisin et al., 2016).

GABAergic neurons in the DR form a large population of cells located mostly lateral to serotonergic neurons (Calizo et al., 2011; Day et al., 2004). Glutamate decarboxylase (GAD), the enzyme responsible for GABA synthesis has two isoforms, GAD65 and GAD67 (Soghomonian and Martin, 1998). The subcellular localization of GAD expression in the DR follows the same general pattern seen across the brain, with GAD65 localized to axon terminals and GAD67 located in the neuronal cell body (Shikanai et al., 2012b; Soghomonian and Martin, 1998). In mouse, GAD67-positive cells in DR have been shown to project to the PFC, nucleus accumbens, and lateral hypothalamus (Bang and Commons, 2012); we wanted to determine if GAD67-positive DR neurons project to the mPFC and LGN in the rat and whether those cells are purely GABAergic or if GAD67 is co-expressed with 5-HT.

NO is a free radical gas with an emerging role in many kinds of neuronal signaling, including responses to stress (Chen et al., 2015; Vincent, 2010). Neuronal nitric oxide synthase (nNOS) and NADPH-diaphorase (NADPH-d) are both used as makers for NO (Lu et al., 2010; Wotherspoon et al., 1994). nNOS is expressed in the cell bodies of DR neurons, and the co-localization of nNOS with serotonergic markers is frequently observed in the midline sub-regions of the DR (Vasudeva et al., 2011). Inhibitors of NOS administered locally within the DR have been shown to have antidepressant activity in rodent models of depression (Spiacci et al., 2008) and NADPH-d levels increase in the DR after exposure to several different acute stressors (Okere and Waterhouse, 2006a; Okere and Waterhouse, 2006b). Those findings linking NO in the DR to stress responses and depressive behaviors, in which 5-HT is also implicated, suggest that characterizing the relationship between NO and 5-HT in specified subsets of DR projection neurons may have clinical value.

We focused on the neurochemical properties of DR neurons projecting to the medial prefrontal cortex (mPFC), a region responsible for higher-order cognition, emotional processing, and the coordination of behavioral responses to stress (Ongur and Price, 2000; Quirk and Beer, 2006). The activity of the mPFC is often altered in depressed patients and reduced serotonin transmission in mPFC is associated with negative affective bias and increased risk of suicide (Johnstone et al., 2007; Leyton et al., 2006; Phillips et al., 2015). Together, this suggests that DR 5-HT neurons targeting mPFC represent a pathway relevant to mood disorders. To determine if the combination of neurotransmitters expressed by mPFC-projecting DR neurons is target-specific, we also examined neurons projecting to the LGN, a subcortical structure that relays visual sensory information from the retina to the cortex (Sherman and Koch, 1986). We chose neurons targeting the LGN for comparison because visual sensory circuits are functionally distinct from the cognitive and emotional circuits within the mPFC.

2. Results

2.1 Anatomical distribution and serotonergic identity of labeled DR neurons

Cell counts were collected from 12 animals, six that received Fluoro-Gold (FG) injections into mPFC and six that received FG injections into LGN. A representative mPFC injection site is shown in Figure 1A. In general, mPFC projecting neurons within the DR were located near the midline and predominantly ipsilateral to the injection site. They were distributed in

the dorsomedial and ventromedial sub-regions of the DR, with a slight general preference for the ventromedial region (Figure 1C, 1E). Along the rostrocaudal axis, the number of mPFC-projecting cells at each level was roughly proportional to the cross-sectional area of the nucleus in the coronal plane, with the most labeled cells found approximately 7.8 mm caudal to bregma. Figure 1B shows an injection of FG into the LGN. Approximately 60% of LGN-projection neurons were located in the lateral wings of the DR; the other 40% were distributed within the dorsomedial and ventromedial sub-regions, with a slightly higher concentration of labeled cells generally found in the dorsomedial region (Figure 1D, 1F). LGN-projecting cells were located primarily ipsilateral to the injection site.

To determine the overall serotonergic component of the DR projections to each terminal field we pooled the counts of neurons containing serotonergic markers across all mPFC cases and all LGN cases separately. We found that 90% of the DR neurons projecting to the mPFC (2018/2238 cells) and 95% of neurons projecting to LGN (2009/2117 cells) had positive immunoreactivity for either TPH or 5-HT. The association between serotonergic projections and projection target was significant ($\chi^2 = 34.25$, $p < 0.0001$).

2.2 VGLUT3 expression in labeled DR neurons

VGLUT3 was highly expressed in neuronal cell bodies throughout the entire DR. At low power, frequent co-localization of VGLUT3 and TPH was observed (Figure 2A–C). Figure 2D shows representative images of labeled DR neurons stained for TPH and VGLUT3. 3% of the mPFC-projecting cells did not show positive immunoreactivity for TPH or VGLUT3 (FG-only), 9% were only positive for VGLUT3, 2% were only positive for TPH, and 86% were positive for both TPH and VGLUT3 (Table 1). While most mPFC-projecting cells with different immunoreactivities were spread evenly throughout the nucleus, most of the VGLUT3-only cells were concentrated in the most rostral sections of the DR (95%, 71/75 of these cells were located in the rostral third of the nucleus). Among neurons projecting to LGN, 3% expressed FG only, 4% expressed VGLUT3 only, 1% expressed TPH only, and 92% expressed TPH and VGLUT3 (Table 2). VGLUT3 was frequently co-expressed in TPH-positive neurons projecting to the mPFC (98%, 698/712 cells) and also in TPH-positive neurons projecting to the LGN (98%, 722/733 cells). A chi-square test of independence determined that there was no significant association between VGLUT3 co-expression and projection target ($\chi^2 = 0.23$, $p = 0.63$). There was also no association between VGLUT3 co-expression and midline vs lateral location of LGN-projecting serotonergic neurons ($\chi^2 = 1.71$, $p = 0.19$).

2.3 GAD67 expression in labeled DR neurons

GAD67 expression was concentrated lateral to serotonin-containing neurons at all levels of the DR (Figure 3A–C) and was rarely observed in labeled neurons (Figure 3D). None of the mPFC-projecting neurons expressed GAD67 only, 92% expressed 5-HT only, and 0.1% expressed both GAD67 and 5-HT (Table 3). Approximately 8% of the mPFC-projecting neurons expressed neither GAD67 nor 5-HT (FG-only); most of these FG-only neurons (92%, 57/62) were concentrated in the rostral one-third of the nucleus, while cells with other immunoreactive profiles were evenly distributed throughout the DR without obvious clustering or segregation. 4% of the LGN-projecting neurons were FG-only, 0.1% expressed

GAD67 only, 95% expressed 5-HT only, and 1% expressed both 5-HT and GAD67 (Table 4). A chi-square test of independence determined that there was a significant association between GAD67 co-expression and projection target ($\chi^2 = 3.9$, $p = 0.049$). There was no association between GAD67 co-expression and midline vs lateral location of LGN-projecting serotonergic neurons ($\chi^2 = 0.031$, $p = 0.86$).

2.4 nNOS expression in labeled DR neurons

The pattern of nNOS expression in the DR differed along the rostrocaudal extent of the nucleus. At the rostral (Figure 4A) and intermediate (Figure 4B) levels of the DR, nNOS expression was observed near the midline and frequently co-localized with TPH in neuronal cell bodies, particularly in the ventromedial subdivision of the nucleus and in a cluster of cells just ventral to the cerebral aqueduct. At those levels, nNOS expression was weaker in the lateral wings, and co-localization of nNOS and TPH was rarely observed in that region. In the caudal portion of the DR (Figure 4C), nNOS had limited overlap with the midline serotonergic neurons, but it was highly expressed in the cholinergic neurons of the lateral dorsal tegmental nucleus located lateral to the midline 5HT-containing cells. Representative images of nNOS and TPH immunoreactivity in DR neurons are shown in Figure 4D.

The immunoreactive profiles of mPFC-projecting neurons were as follows: 9% expressed neither nNOS nor TPH (FG-only), 1% expressed nNOS only, 36% expressed TPH only, and 54% expressed both TPH and nNOS (Table 3). As seen in tissue stained for 5-HT and GAD67, the FG-only neurons were clustered towards the rostral third of the nucleus (98%, 54/55 cells). Of neurons projecting to the LGN, 1% expressed neither nNOS nor TPH, 3% expressed nNOS only, 75% expressed TPH only, and 21% expressed TPH and nNOS. nNOS was co-expressed in 60% of the TPH-positive neurons projecting to mPFC (343/574 cells) and in 21% of the TPH-positive neurons projecting to LGN (140/637 cells); there was a significant association between nNOS co-expression and projection target ($\chi^2 = 178.1$, $p < 0.0001$).

Within the LGN-projecting population, 41% (120/295 cells) of the TPH-expressing neurons in the dorsomedial and ventromedial sub-regions were nNOS-positive, while only 6% (20/342 cells) of the TPH-expressing neurons in the lateral wings were nNOS-positive. The association between nNOS co-expression and midline vs lateral location of LGN-projecting cells was significant ($\chi^2 = 110.0$, $p < 0.0001$). When mPFC-projecting cells were compared to only LGN-projecting cells located within midline ($\chi^2 = 27.7$, $p < 0.0001$) or lateral ($\chi^2 = 258.07$, $p < 0.0001$) sub-regions of the DR, the association between nNOS co-expression and efferent target was significant in both cases. Some dorsoventral segregation of DR neurons projecting to mPFC vs LGN was observed in midline regions of the DR. In all mPFC-injected cases, the proportion of TPH/nNOS double-positive cells located in the dorsomedial and ventromedial sub-regions were approximately 25% and 75%, respectively. In four LGN-injected cases, the labeled cells were nearly evenly distributed between dorsomedial and ventromedial regions, while in two cases almost all the labeled cells were located in the dorsomedial region.

3. Discussion

3.1 Serotonergic identity of labeled neurons

Serotonin-containing neurons that project from the DR to the mPFC have previously been identified using both retrograde (Del Cid-Pellitero and Garzon, 2011; Fernandez et al., 2016; Lu et al., 2010; Meloni et al., 2008; Van Bockstaele et al., 1993) and anterograde tracing approaches (Gagnon and Parent, 2014; Muzerelle et al., 2014; Vertes, 1991). Our finding that 90% of the DR neurons projecting to mPFC are serotonergic aligns with several studies which reported percentages of 74–92% for this class of neurons (Fernandez et al., 2016; Lu et al., 2010; Meloni et al., 2008); however, there are two studies that found serotonergic proportions of 42% (Del Cid-Pellitero and Garzon, 2011) and 34% (Van Bockstaele et al., 1993). In the work by Del Cid-Pellitero et al, the tracer injections were directed at anterior cingulate cortex (ACC), medial orbital cortex, and prelimbic (PL) cortex, while ours were only directed at the PL and infralimbic (IL) cortices. As the sub-regions of PFC are thought to regulate distinct aspects of cognition and emotional processing (Dalley et al., 2004; Kesner and Churchwell, 2011; Sul et al., 2010) they may require different degrees of serotonergic modulation; therefore, the difference in the reported proportion of serotonergic projection neurons between that study and ours may be due to injection targeting. This possibility is supported by the fact that significant differences have been described in the number and rostrocaudal distribution of DR neurons projecting to PL/IL, ACC, and orbitofrontal cortex (Chandler et al., 2013). Van Bockstaele et al. included neurons located in the most caudal regions of the DR in their analysis. A recent review by Commons suggests that the serotonergic neurons comprising the caudal DR, designated as B6 by Dahlström and Fuxe, are more genetically and functionally similar to serotonergic neurons of the median raphe (MR) nucleus than to those in the rest of the DR (Commons, 2016). It is possible that the inclusion of those caudal DR neurons accounts for the different proportions of mPFC-projecting serotonergic cells reported by Van Bockstaele et al. and our current result.

Early retrograde tracing studies identified DR neurons that project to LGN (Pasquier and Villar, 1982; Villar et al., 1988; Waterhouse et al., 1993). Although the neurochemical identity of those neurons was either not assessed or the findings were not evaluated quantitatively, serotonergic projections from DR to LGN have been demonstrated in anterograde tracing studies (Muzerelle et al., 2014; Vertes et al., 2010). The general distribution of LGN projecting DR neurons that we observed, i.e. a majority of labeled neurons located in the lateral wing ipsilateral to the injection site and fewer located in in midline regions, corresponds with the pattern described in those earlier studies.

3.2 VGLUT3

The majority of FG-labeled neurons in the DR displayed VGLUT3 immunoreactivity and VGLUT3 was observed in 98% of serotonergic projection neurons, regardless of efferent target. The only other study examining VGLUT3 in serotonergic neurons specifically projecting to mPFC found that only 15% (3/20 cells) contained VGLUT3 (Fernandez et al., 2016). However, the work by Fernandez et al. differed from ours in several important ways. The study was conducted in mouse, VGLUT3 expression was determined by RT-PCR on the

aspirated cellular contents of neurons that had been used for electrophysiological recordings, and six of the 5-HT projection cells to mPFC were located in the MR. The high proportion of cells staining positive for both VGLUT3 and TPH that we observed corresponds well with several previous studies showing that VGLUT3 mRNA (Gras et al., 2002) and protein (Calizo et al., 2011; Gagnon and Parent, 2014; Hioki et al., 2004; Mintz and Scott, 2006; Shutoh et al., 2008) is found in the cell bodies of nearly all DR 5-HT neurons.

In contrast to the body of literature describing widespread co-localization of 5-HT and VGLUT3 throughout the DR, there are reports of VGLUT3 expression largely restricted to neurons located within midline DR sub-regions (Commons, 2009; Hioki et al., 2010). One of these reports found that VGLUT3-positive neurons lacking 5-HT were concentrated near the midline of the DR (Commons, 2009). Notably, 5-HT/VGLUT3 double-positive neurons, which constituted approximately 90% of our labeled cells, were excluded from that 2009 study and may account for the reported differences in VGLUT3 expression. A study by Hioki et al. found that among DR 5-HT neurons, VGLUT3 mRNA was expressed by approximately 80% of the cells located in midline sub-regions vs only 4% of the cells in the lateral wings (Hioki et al., 2010). Interestingly, the authors of Gras et al., 2002 reported the presence of VGLUT3 mRNA in all 5-HT neurons throughout the DR, but also noted a higher density of VGLUT3 mRNA in midline regions than in the lateral wings. There is notable variability in the level of VGLUT3 signal within individual DR neurons as detected by immunohistochemistry—in one study VGLUT3 immunoreactivity was described as ranging from “barely detectable” to “clearly defining the entire extent of the cell soma” (Mintz and Scott, 2006), while a separate report concluded that all DR 5-HT neurons contained “various amounts of VGLUT3-positive particles” (Shutoh et al., 2008). The wide range of VGLUT3 signal within DR neurons may increase the potential for different interpretations of positive immunoreactivity across researchers and may contribute to the divergent reports of VGLUT3 expression in the DR.

The functional implications of VGLUT3 in serotonergic neurons are unclear, although several possibilities have been suggested: 1) glutamate is used as a transmitter in 5-HT neurons—either via co-release with 5-HT at the same terminals (Gagnon and Parent, 2014) or via segregated release from different terminals (Amilhon et al., 2010), 2) VGLUT3 enhances the efficiency of serotonin signaling by facilitating vesicular packaging of 5-HT (Amilhon et al., 2010), and 3) VGLUT3 may adjust the ratio of synaptic transmission to volume transmission along serotonergic axons by promoting the formation of synaptic specializations (Gagnon and Parent, 2014; Voisin et al., 2016). A study using cultured mesopontine 5-HT neurons found that those from a VGLUT3 knockout mouse had a significantly lower basal survival rate compared to serotonergic cells from wild-type littermates (Voisin et al., 2016). The authors of that study suggest that VGLUT3 may regulate serotonergic neuronal development or confer general fitness to 5-HT neurons; such functions could explain the presence of VGLUT3 in nearly all DR 5-HT cell bodies that we observed (Voisin et al., 2016).

We also identified a group of cells that may represent a population of non-serotonergic neurons projecting specifically to mPFC that use glutamate as their primary transmitter. In samples from mPFC-injected animals that were stained for TPH and VGLUT3, the

VGLUT3-only neurons were primarily located along the midline in the most rostral 280 μm of the DR and comprised 7% of the total labeled neurons. Interestingly, in samples stained for 5-HT/GAD and TPH/nNOS there were groups of FG-only neurons that accounted for 8% and 9% of the respective projections to mPFC. These were located in the same rostral midline location as the VGLUT3-only group. The overlap in proportion and location of these three groups may indicate that they are the same population of neurons which express VGLUT3, but are negative for all other markers that we examined. Though dopaminergic neurons are known to express VGLUTs, and the location of our VGLUT3-only population is similar to that of dopaminergic neurons in the DR, sometimes referred to as the dorsocaudal extension of the A10 group (Dougalis et al., 2012), there does not seem to be overlap between VGLUT3 and tyrosine hydroxylase (the rate-limiting enzyme of dopamine synthesis) in DR neurons (Hioki et al., 2010). The non-serotonergic, VGLUT3-positive DR projection system is being actively explored and several studies using retrograde or anterograde tracing have found strong VGLUT3-only projections to the ventral tegmental (VTA) and hypothalamus, as well as lesser projections to other regions including ventral palladium and medial septum (Hioki et al., 2010; Jackson et al., 2009; Qi et al., 2014). While non-serotonergic projections from DR to PFC have been described, our report is the first to specifically identify non-serotonergic, VGLUT3-positive neurons projecting to PL and IL regions of the mPFC (Bang and Commons, 2012; McDevitt et al., 2014). No rostral clusters of VGLUT3-only or FG-only neurons were observed in samples from LGN-injected animals, suggesting the glutamatergic signals originating from the DR are of specific import to the mPFC. Since many of the DR VGLUT3-only projections targeting VTA have been implicated in reward signaling, it is possible that the VGLUT3-only cells we observed may regulate mPFC processes such as reward value coding and determination of behavioral responses to appetitive stimuli (Richard and Berridge, 2013).

3.3 GAD67

We found very few cells that contained GAD67. A study that examined DR projections to mPFC in a GAD67-GFP mouse line found that 16% of the projection neurons were GAD67-positive, although whether those cells expressed serotonergic markers was not evaluated (Bang and Commons, 2012). Many of those mPFC-projecting cells were interspersed amidst the fibers of the MLF, a region that we did not include in our counts. The low number of projection neurons displaying 5-HT and GAD67 co-localization agrees with previous reports that neurons positive for both 5-HT and GAD67 make up a very small proportion of all DR neurons (Hioki et al., 2010; Shikanai et al., 2012a; Stamp and Semba, 1995). Although we found a significant association between projection target and co-expression of GAD67 in serotonergic neurons, it is difficult to extrapolate the functional significance of such a low number of cells. While our data suggests that 5-HT/GABA interactions within DR neurons projecting to mPFC or LGN are unlikely in adult rats, the possibility that such interactions may have a temporally-specific role during development is supported by a study that found that the number of 5-HT/GAD67-positive cells in rat DR changes significantly between 2, 4, and 8 weeks of age (Shikanai et al., 2012a).

3.4 nNOS

A previous report of DR projections to mPFC found that 83% of the serotonergic cells were nNOS-positive (Lu et al., 2010). Although that study and ours reported similar proportions of TPH and nNOS double-positive neurons (62% vs 54%), they observed fewer TPH-only neurons (12% vs 36%) (Lu et al., 2010). These differences may be due to sex (Lu et al. used female Long-Evans rats), or because of technical differences including the use of different antibodies. The possibility of sex differences in the neurochemistry of DR 5-HT neurons, especially in cells projecting to mPFC or other circuits that regulate mood, merits further exploration because of the gender disparity in the lifetime prevalence of affective disorders in the human population (Kessler et al., 2005). Previous studies have identified distinct mediolateral differences in the proportion of DR serotonergic neurons that express NOS, ranging from 70–80% in midline regions to 2.5–10% in the LW (Johnson and Ma, 1993; Simpson et al., 2003). When we compared the nNOS-TPH co-expression in mPFC-projecting cells (which were entirely located in midline regions) to only LGN-projecting neurons found in midline regions, and separately to LGN-projecting neurons in the LW; the association was significant in both cases. This suggests that the target-specific difference in nNOS co-expression is not simply the result of the regional disparity in LGN-projecting cells.

Nitric oxide has been implicated in activity-dependent plasticity due to the functional coupling of nNOS with glutamatergic NMDA receptors (Garthwaite, 2016). Both nNOS and NMDA receptors are tethered to postsynaptic density protein 95 and calcium entry through NMDA receptors activates nNOS as a result of the physical proximity between the two proteins (Garthwaite, 2016). NO frequently acts as a retrograde messenger, which, when released from activated postsynaptic neurons, can enhance subsequent presynaptic signals from both glutamatergic and GABAergic terminals (Haghikia et al., 2007; Yamamoto et al., 2015). It is possible that the greater presence of nNOS we observed in mPFC-projecting 5-HT neurons allows for more dynamic regulation of mPFC circuitry.

NOS expression has also been observed in the varicosities of serotonergic axons that originate in the DR, and therefore NO likely influences DR efferent targets in addition to its potential role as a feedback regulator of 5-HT neurons (Lu et al., 2010; Simpson et al., 2003). The high proportion of fibers in mPFC that co-express nNOS and SERT suggests that interactions between 5-HT with NO may be particularly important in that region (Lu et al., 2010). NOS has also been shown to physically couple with SERT which means that it may influence extracellular 5-HT levels in terminal fields (Chanrion et al., 2007).

3.5 Functional considerations

The rodent mPFC is implicated in several correlates of human emotional processing, including contextual fear learning, assessment of stressor controllability, and the implementation of behavioral coping strategies in response to challenge (Etkin et al., 2011; Quirk and Beer, 2006). In addition to the functional homology, similarities in network connectivity between the human and rodent mPFC indicate that DR 5-HT neurons targeting the mPFC in rodents constitute a valuable pathway for the study of affective disorders (Etkin et al., 2011; Quirk and Beer, 2006).

In humans, the mPFC is responsible for both cognitive processes, such as attention and working memory, as well as the regulation of limbic circuits and the generation of behavioral responses to emotional and rewarding stimuli (Etkin et al., 2011; Ongur and Price, 2000). mPFC dysfunction, in the form of reduced metabolic activity (especially in response to negative stimuli), or reduced gray matter volume has been reported in imaging studies of depressed subjects relative to healthy subjects (Drevets et al., 2008; Fales et al., 2008; Siegle et al., 2007). The mPFC is thought to exert top-down inhibitory control over the processing of negative emotional stimuli in the amygdala, and mPFC dysfunction may contribute to the negative affective bias characteristic of depression (Drevets et al., 2008; Lemogne et al., 2012; Phillips et al., 2015). Serotonin transmission is known to regulate emotional processing; within the mPFC specifically, reduced serotonin receptor type 2A (5-HT_{2A}) binding correlates with amygdala hyperactivity and also with ratings of hopelessness in suicidal patients (Aznar and Klein, 2013; Fisher et al., 2009; van Heeringen et al., 2003). Together, this evidence indicates 5-HT tone in mPFC has an important role in emotional status and that the co-transmitter profile of mPFC-projecting DR 5-HT neurons has important implications for the pathophysiology of mood disorders. For example, the greater proportion of nNOS expression observed in mPFC-projecting vs LGN-projecting DR 5-HT cells may represent a potential mechanism underlying the strong correlation between stressful events and the onset and recurrence of depressive episodes (Kendler et al., 1999). Glucocorticoids promote the synthesis of and release of NO from magnocellular neurons in the hypothalamus; in that circuit, NO—acting as a retrograde messenger—reduces the activity of the magnocellular neurons by enhancing presynaptic GABA release (Di et al., 2009). If a similar mechanism exists within the DR, it could result in stress-induced hypofunction of 5-HT/nNOS cells and a corresponding decrease in serotonergic transmission in structures such as the mPFC that receive strong projections from 5-HT/nNOS neurons.

3.6 Conclusions

Four main conclusions stem from this work. 1) VGLUT3 was highly expressed in DR projection neurons and the proportion of serotonergic neurons containing VGLUT3 was nearly identical in both mPFC- and LGN-projecting cells. 2) A group of putative glutamatergic neurons located in the rostral DR express VGLUT3 without TPH and specifically project to the mPFC. 3) There was a significant association between GAD67 co-expression and efferent target in serotonergic projection neurons, but 5-HT/GAD67 double-positive cells were rarely observed. 4) There was a significant association between nNOS co-expression and projection target; nNOS was expressed in a greater proportion of the DR 5-HT neurons projecting to mPFC than to LGN.

4. Experimental Procedures

4.1 Retrograde tracing

The Drexel University College of Medicine Institutional Animal Care and Use Committee approved all animal procedures and protocols. Young-adult, male Sprague-Dawley rats (Taconic Biosciences, Hudson, NY) received stereotaxically guided injections of Fluoro-Gold (Fluorochrome Inc., Denver, CO) into the mPFC or LGN. Anesthesia was induced and

maintained via isoflurane inhalation at concentrations of 4% and 2.5% isoflurane (v/v), respectively, in 95% oxygen and 5% carbon dioxide. Throughout each surgical procedure, body temperature was monitored and maintained at 37°C using a water-circulating heating pad. Injection coordinates were based on Paxinos and Watson, 1997. The following coordinates for each target region are listed, relative to bregma, in the anteroposterior (AP), mediolateral (ML), and dorsoventral (DV) planes. mPFC coordinates: AP +3.2 mm, ML ±1.3 mm, DV −4.5 mm. LGN coordinates: AP −4.8 mm, ML ±3.9 mm, DV −4.6 mm. DV measurements were made from the skull surface and, when targeting the mPFC, at an angle of 10° from perpendicular to the skull. All injections were made into the left hemisphere. 0.2 μl pressure injections of a 3% FG solution (FG dissolved in distilled water) were made using a Hamilton Neuros syringe with a 33-gauge stainless steel, non-beveled needle. The syringe was manually dispensed using a Kopf Model 5000 microinjection unit to achieve an injection rate of 0.036 μl/min. The syringe was left in place for ten minutes after completion of each injection to allow for tracer diffusion. After a survival period of seven days the rats were sacrificed and brain tissue was processed for immunohistochemistry.

4.2 Tissue processing

Rats were deeply anesthetized with isoflurane and transcardially perfused with 240 ml of normal saline solution containing heparin (0.9% sodium chloride and 10 U/ml heparin in distilled water) followed by 240 ml of 4% paraformaldehyde in 0.1 M phosphate buffer (4% PFA). Brain tissue was extracted, post-fixed in 4% PFA for 24 h, then cryoprotected in 20% sucrose solution (sucrose in 0.1 M phosphate buffer) for 48 h. The brains were frozen on dry ice, sectioned along the coronal plane using a Leica freezing sliding microtome, and collected into 0.01 M phosphate-buffered saline (PBS). Injection sites were sectioned at a thickness of 80 μm and collected in a 1:3 series, while brainstem tissue containing the DR was sectioned at 40 μm and collected in a 1:6 series. Immunohistochemical staining was performed on free-floating sections of brainstem tissue.

4.3 Antibody characterization

Mouse monoclonal anti-tryptophan hydroxylase antibody (Sigma-Aldrich Cat# T0678, RRID: AB_261587). The antibody was raised against recombinant rabbit TPH (manufacturer's product information). Antibody specificity was confirmed by the manufacturer using western blot, which resulted in a single 55 kDa band characteristic of TPH. The antibody has been widely used as a marker of serotonin neurons and the staining pattern seen in our study matches known serotonergic neurons as well as previous studies which used this antibody (Liu and Wong-Riley, 2010; Rosin et al., 2006).

Rabbit polyclonal anti-serotonin antibody (ImmunoStar Cat# 20080, RRID: AB_572263). 5-HT conjugated to bovine serum albumin (BSA) was used as the immunogen. The manufacturer confirmed antibody specificity by preadsorption with 25 μg/ml serotonin-BSA, which completely eliminated the signal. Preadsorption testing with several compounds structurally-related to serotonin (including dopamine) found no cross-reactivity (manufacturer's product information). The staining pattern we observed corresponds with known locations of serotonergic neurons and also matches those of previous studies that used this antibody (Calizo et al., 2011; Muller et al., 2007; Suzuki et al., 2015).

Rabbit polyclonal anti-VGLUT3 antibody (Abcam Cat# ab23977, RRID: AB_2270290). A synthetic peptide sequence from the C-terminus of rat VGLUT3 was used as the immunogen (manufacturer's product information). Western blot testing found that the antibody labels a single band corresponding to VGLUT3 and has no cross-reactivity with VGLUT1 or VGLUT2 (manufacturer's product information). The staining pattern observed in our study was consistent with previous studies examining VGLUT3 in DR (Calizo et al., 2011; Gagnon and Parent, 2014; Hioki et al., 2004).

Mouse monoclonal anti-GAD67 antibody (Millipore Cat# MAB5406, RRID: AB_2278725). The antibody was raised against recombinant whole GAD67 protein (manufacturer's product information). Testing by the manufacturer found that the antibody labeled a single band on western blot consistent with GAD67 (confirmed by (Ito et al., 2015)) and shows no cross reactivity with GAD65. Antibody specificity was further confirmed by preadsorption of the antibody with recombinant rat GAD67, which completely abolished the signal (Ito et al., 2015). This antibody has been well-established as a marker of GABA-producing neurons (Fong et al., 2005). The staining pattern we observed matched those of previous studies (Calizo et al., 2011; Fu et al., 2010).

Rabbit polyclonal anti-nNOS antibody (ImmunoStar Cat# 24431, RRID: AB_572255). The immunogen used to generate this antibody was a synthetic peptide sequence from the N-terminus of human nNOS coupled to keyhole limpet hemocyanin (manufacturer's product information). Manufacturer testing found that the antibody specifically labeled a 155 kDa band characteristic of nNOS, the antibody showed no cross-reactivity with other forms of NOS, and pre-adsorption with the manufacturer's control peptide (5 μg/ml) abolished all staining. Previous studies have shown that the staining pattern of this antibody corresponds with known nitrergic neurons; the staining we observed matched the established patterns (Piskuric et al., 2011; Stillman et al., 2009).

The anti-TPH and anti-GAD67 antibodies are not compatible with each other for co-localization experiments because they were both raised in the same host species (mouse); therefore, the rabbit anti-5-HT antibody was used as an alternative marker for serotonergic neurons in double-labeling experiments with the anti-GAD67 antibody. While the two antibodies we used to identify serotonergic neurons (anti-TPH and anti-5-HT) have different levels of sensitivity, we accounted for this by conducting preliminary experiments in which we identified the concentrations of each antibody that produced the best signal to noise ratio and similar numbers of immunoreactive cells in the DR. Using the optimized concentrations, we found an average 111 immunoreactive cells per case (24 cases) using the anti-TPH antibody and 114 immunoreactive per case (12 cases) using the anti-5-HT antibody, which indicated to us that the different levels of antibody sensitivity were well controlled.

4.4 Immunohistochemistry

The sections were washed in PBS (three 10-minute washes) and incubated in PBS with 0.3% Triton X-100 (PBST) and 5% normal goat serum (NGS) for 1 h. Next, sections were transferred to a solution containing primary antibodies and 1% NGS in PBST overnight (18 h) at 4°C. Following three 10-minute washes in PBS, the tissue was incubated with secondary antibodies in PBST for 1 h. The secondary antibodies used were goat anti-rabbit

Alexa Fluor 555 and goat anti-mouse Alexa Fluor 488 (Molecular Probes, Eugene, OR). The sections were then washed in PBS and each series was mounted onto a gelatin-coated slide. Once dry, the tissue was cleared by dipping the slides in PBS for 60 s followed by xylene for 30 s. The slides were cover-slipped with ProLong Diamond anti-fade mounting media (Invitrogen, Carlsbad, CA). The neurochemical markers used were TPH or serotonin itself (5-HT) for serotonin, VGLUT3 for glutamate, GAD67 for GABA, and nNOS for nitric oxide. Each series used for data collection was stained with one of three pairs of primary antibodies and the corresponding secondary antibodies (Table 7). Preadsorption of the VGLUT3 antiserum with an excess (25 μg) of its control peptide (Abcam, ab223018) resulted in the elimination of VGLUT3 signal. To control for non-specific labeling by secondary antibodies, some series were subjected to the same staining procedures except that the primary antibodies were excluded from the overnight incubation.

4.5 Verification of injection sites

Sections containing the mPFC and LGN of rats injected with FG were examined and photographed with a Leica DM RBE fluorescence microscope and QImaging Retiga EXi Camera (Model RGB-MS-C) to determine injection accuracy and the extent of tracer diffusion. mPFC injections were considered acceptable if they were contained within the prelimbic and infralimbic cortices with limited extension into dorsal peduncular cortex and anterior cingulate cortex. Injections contained within the dorsal lateral geniculate nucleus, intergeniculate leaflet, or ventral lateral geniculate nucleus were considered acceptable for LGN. If an injection was off-target or the tracer had diffused significantly beyond the borders described above, the corresponding DR sections from that animal were excluded from data collection and analysis. In one of the LGN cases, FG spread into the hippocampus just dorsal to the LGN, but because the serotonin projections to that region arise primarily from the median raphe nucleus, with only sparse contributions from DR (Muzerelle et al., 2014; Vertes, 1991), this case was considered acceptable.

4.6 Cell counting

Counts were collected from an average of eight sections (240 μm apart) per series. Brainstem sections were viewed with a Leica DM RBE fluorescence microscope and photographed using a QImaging Retiga EXi digital camera. Sections were scanned at 40x magnification to identify FG-labeled neurons within the DR. At seven days post-injection, FG accumulation in the cytoplasm produces bright labeling that fills the cell body and extends into dendrites. Each FG-positive neuron was individually viewed at 63x magnification through selective fluorescence filters to determine its immunoreactivity. Labeled neurons were classified by their immunoreactivity and tallied to determine the total number of neurons expressing each possible combination of neurochemical markers in each series. Representative neurons were sequentially photographed through three fluorescence filters and QCapture Pro 6 software (QImaging, BC, Canada) was used to generate composite overlays of those images for each cell. The low magnification photomicrographs (Figures 2–4, A–C) were adjusted for brightness and contrast using the image editing software GIMP 2.8.

While immunohistochemistry (IHC) is an excellent tool for examining the anatomical distribution and cellular co-localization of target proteins, other techniques such as ELISA and western blot are more sensitive measures of protein expression; therefore, the absence of staining within our study is not intended to definitively exclude the presence of the corresponding neurochemical marker.

4.7 Analysis of immunohistochemical data

The counts from six series of brainstem tissue (one series from each mPFC-injected animal) were tabulated and totaled for each combination of neurochemical markers (TPH/VGLUT3, 5-HT/GAD67, and TPH/nNOS). The totals from each immunoreactivity category were then expressed as a percentage of the total number of labeled neurons. The same process was used to generate cell count tables for LGN-injected cases. To evaluate co-transmitter expression in serotonergic neurons, we identified the total number of double-positive neurons (cells that expressed the serotonin marker and also expressed VGLUT3 or GAD67 or nNOS) and the total number of serotonergic neurons for each combination of transmitters and each target structure; those values were used to construct 2×2 contingency tables. For each contingency table, a chi-square test of independence was used to determine if transmitter co-localization was dependent on projection target. The significance level for the chi-square test was set at $p = .05$, and Yates' continuity correction was applied.

Acknowledgments

The authors would like to thank Dr. Brian Clark for his assistance with statistical analysis and his comments on the manuscript. This work was supported by the National Institutes of Health R01 MH1011778 to BDW.

Abbreviations

DR	dorsal raphe nucleus
LW	lateral wings of the dorsal raphe nucleus
mPFC	medial prefrontal cortex
LGN	lateral geniculate nucleus
MLF	medial longitudinal fasciculus
TPH	tryptophan hydroxylase
VGLUT3	vesicular glutamate transporter 3
GAD67	glutamate decarboxylase 1
nNOS	neuronal nitric oxide synthase

References

Amilhon B, Lepicard E, Renoir T, Mongeau R, Popa D, Poirel O, Miot S, Gras C, Gardier AM, Gallego J, Hamon M, Lanfumey L, Gasnier B, Giros B, El Mestikawy S. VGLUT3 (vesicular glutamate transporter type 3) contribution to the regulation of serotonergic transmission and anxiety. J Neurosci. 2010; 30:2198–210. [PubMed: 20147547]

Aznar S, Klein AB. Regulating prefrontal cortex activation: an emerging role for the 5-HT(2)A serotonin receptor in the modulation of emotion-based actions? Mol Neurobiol. 2013; 48:841–53. [PubMed: 23696058]

Baker KG, Halliday GM, Hornung JP, Geffen LB, Cotton RG, Tork I. Distribution, morphology and number of monoamine-synthesizing and substance P-containing neurons in the human dorsal raphe nucleus. Neuroscience. 1991; 42:757–75. [PubMed: 1720227]

Bang SJ, Commons KG. Forebrain GABAergic projections from the dorsal raphe nucleus identified by using GAD67-GFP knock-in mice. J Comp Neurol. 2012; 520:4157–67. [PubMed: 22605640]

Calizo LH, Akanwa A, Ma X, Pan YZ, Lemos JC, Craige C, Heemstra LA, Beck SG. Raphe serotonin neurons are not homogenous: electrophysiological, morphological and neurochemical evidence. Neuropharmacology. 2011; 61:524–43. [PubMed: 21530552]

Chandler DJ, Lamperski CS, Waterhouse BD. Identification and distribution of projections from monoaminergic and cholinergic nuclei to functionally differentiated subregions of prefrontal cortex. Brain Res. 2013; 1522:38–58. [PubMed: 23665053]

Chanrion B, Mannoury la Cour C, Bertaso F, Lerner-Natoli M, Freissmuth M, Millan MJ, Bockaert J, Marin P. Physical interaction between the serotonin transporter and neuronal nitric oxide synthase underlies reciprocal modulation of their activity. Proc Natl Acad Sci U S A. 2007; 104:8119–24. [PubMed: 17452640]

Chen HJ, Spiers JG, Sernia C, Lavidis NA. Response of the nitrergic system to activation of the neuroendocrine stress axis. Front Neurosci. 2015; 9:3. [PubMed: 25653586]

Commons KG, Beck SG, Bey VW. Two populations of glutamatergic axons in the rat dorsal raphe nucleus defined by the vesicular glutamate transporters 1 and 2. Eur J Neurosci. 2005; 21:1577–86. [PubMed: 15845085]

Commons KG. Locally collateralizing glutamate neurons in the dorsal raphe nucleus responsive to substance P contain vesicular glutamate transporter 3 (VGLUT3). J Chem Neuroanat. 2009; 38:273–81. [PubMed: 19467322]

Commons, KG. Journal of Comparative Neurology. 2015. Two major network domains in the dorsal raphe nucleus.

Commons KG. Ascending serotonin neuron diversity under two umbrellas. Brain Struct Funct. 2016; 221:3347–60. [PubMed: 26740230]

Dahlström A, Fuxe K. Evidence for the existence of monoamine neurons in the central nervous system. I. Demonstration of monoamines in the cell bodies of brain stem neurons. Acta Physiol Scand Suppl. 1964; (Suppl 232):1–55.

Dalley JW, Cardinal RN, Robbins TW. Prefrontal executive and cognitive functions in rodents: neural and neurochemical substrates. Neurosci Biobehav Rev. 2004; 28:771–84. [PubMed: 15555683]

Day HE, Greenwood BN, Hammack SE, Watkins LR, Fleshner M, Maier SF, Campeau S. Differential expression of 5HT-1A, alpha 1b adrenergic, CRF-R1, and CRF-R2 receptor mRNA in serotonergic, gamma-aminobutyric acidergic, and catecholaminergic cells of the rat dorsal raphe nucleus. J Comp Neurol. 2004; 474:364–78. [PubMed: 15174080]

Del Cid-Pellitero E, Garzon M. Medial prefrontal cortex receives input from dorsal raphe nucleus neurons targeted by hypocretin1/orexinA-containing axons. Neuroscience. 2011; 172:30–43. [PubMed: 21036204]

Di S, Maxson MM, Franco A, Tasker JG. Glucocorticoids regulate glutamate and GABA synapse-specific retrograde transmission via divergent nongenomic signaling pathways. J Neurosci. 2009; 29:393–401. [PubMed: 19144839]

Dougalis AG, Matthews GA, Bishop MW, Brischoux F, Kobayashi K, Ungless MA. Functional properties of dopamine neurons and co-expression of vasoactive intestinal polypeptide in the dorsal raphe nucleus and ventro-lateral periaqueductal grey. Eur J Neurosci. 2012; 36:3322–32. [PubMed: 22925150]

Drevets WC, Price JL, Furey ML. Brain structural and functional abnormalities in mood disorders: implications for neurocircuitry models of depression. Brain Struct Funct. 2008; 213:93–118. [PubMed: 18704495]

Etkin A, Egner T, Kalisch R. Emotional processing in anterior cingulate and medial prefrontal cortex. Trends in cognitive sciences. 2011; 15:85–93. [PubMed: 21167765]

Fales CL, Barch DM, Rundle MM, Mintun MA, Snyder AZ, Cohen JD, Mathews J, Sheline YI. Altered emotional interference processing in affective and cognitive-control brain circuitry in major depression. Biol Psychiatry. 2008; 63:377–84. [PubMed: 17719567]

Fernandez SP, Cauli B, Cabezas C, Muzerelle A, Poncer JC, Gaspar P. Multiscale single-cell analysis reveals unique phenotypes of raphe 5-HT neurons projecting to the forebrain. Brain Struct Funct. 2016; 221:4007–4025. [PubMed: 26608830]

Fisher PM, Meltzer CC, Price JC, Coleman RL, Ziolko SK, Becker C, Moses-Kolko EL, Berga SL, Hariri AR. Medial prefrontal cortex 5-HT2A density is correlated with amygdala reactivity, response habituation, and functional coupling. Cerebral cortex. 2009 pbhp022.

Fong AY, Stornetta RL, Foley CM, Potts JT. Immunohistochemical localization of GAD67-expressing neurons and processes in the rat brainstem: subregional distribution in the nucleus tractus solitarius. J Comp Neurol. 2005; 493:274–90. [PubMed: 16255028]

Fremeau RT Jr, Voglmaier S, Seal RP, Edwards RH. VGLUTs define subsets of excitatory neurons and suggest novel roles for glutamate. Trends Neurosci. 2004; 27:98–103. [PubMed: 15102489]

Fu W, Le Maitre E, Fabre V, Bernard JF, David Xu ZQ, Hokfelt T. Chemical neuroanatomy of the dorsal raphe nucleus and adjacent structures of the mouse brain. J Comp Neurol. 2010; 518:3464–94. [PubMed: 20589909]

Gagnon D, Parent M. Distribution of VGLUT3 in highly collateralized axons from the rat dorsal raphe nucleus as revealed by single-neuron reconstructions. PloS one. 2014; 9:e87709. [PubMed: 24504335]

Garthwaite J. From synaptically localized to volume transmission by nitric oxide. J Physiol. 2016; 594:9–18. [PubMed: 26486504]

Gaspar P, Lillesaar C. Probing the diversity of serotonin neurons. Philos Trans R Soc Lond B Biol Sci. 2012; 367:2382–94. [PubMed: 22826339]

Gras C, Herzog E, Bellenchi GC, Bernard V, Ravassard P, Pohl M, Gasnier B, Giros B, El Mestikawy S. A third vesicular glutamate transporter expressed by cholinergic and serotoninergic neurons. J Neurosci. 2002; 22:5442–51. [PubMed: 12097496]

Haghikia A, Mergia E, Friebe A, Eysel UT, Koesling D, Mittmann T. Long-term potentiation in the visual cortex requires both nitric oxide receptor guanylyl cyclases. J Neurosci. 2007; 27:818–23. [PubMed: 17251421]

Hale MW, Lowry CA. Functional topography of midbrain and pontine serotonergic systems: implications for synaptic regulation of serotonergic circuits. Psychopharmacology (Berl). 2011; 213:243–64. [PubMed: 21088958]

Hioki H, Fujiyama F, Nakamura K, Wu SX, Matsuda W, Kaneko T. Chemically specific circuit composed of vesicular glutamate transporter 3- and preprotachykinin B-producing interneurons in the rat neocortex. Cereb Cortex. 2004; 14:1266–75. [PubMed: 15142960]

Hioki H, Nakamura H, Ma YF, Konno M, Hayakawa T, Nakamura KC, Fujiyama F, Kaneko T. Vesicular glutamate transporter 3-expressing nonserotonergic projection neurons constitute a subregion in the rat midbrain raphe nuclei. J Comp Neurol. 2010; 518:668–86. [PubMed: 20034056]

Ito T, Hioki H, Sohn J, Okamoto S, Kaneko T, Iino S, Oliver DL. Convergence of Lemniscal and Local Excitatory Inputs on Large GABAergic Tectothalamic Neurons. J Comp Neurol. 2015; 523:2277–96. [PubMed: 25879870]

Jackson J, Bland BH, Antle MC. Nonserotonergic projection neurons in the midbrain raphe nuclei contain the vesicular glutamate transporter VGLUT3. Synapse. 2009; 63:31–41. [PubMed: 18925658]

Jacobs BL, Azmitia EC. Structure and function of the brain serotonin system. Physiological reviews. 1992; 72:165–229. [PubMed: 1731370]

Johnson MD, Ma PM. Localization of NADPH diaphorase activity in monoaminergic neurons of the rat brain. J Comp Neurol. 1993; 332:391–406. [PubMed: 8102384]

Johnstone T, van Reekum CM, Urry HL, Kalin NH, Davidson RJ. Failure to regulate: counterproductive recruitment of top-down prefrontal-subcortical circuitry in major depression. J Neurosci. 2007; 27:8877–84. [PubMed: 17699669]

Kendler KS, Karkowski LM, Prescott CA. Causal relationship between stressful life events and the onset of major depression. American Journal of Psychiatry. 1999

Kesner RP, Churchwell JC. An analysis of rat prefrontal cortex in mediating executive function. Neurobiol Learn Mem. 2011; 96:417–31. [PubMed: 21855643]

Kessler RC, Berglund P, Demler O, Jin R, Merikangas KR, Walters EE. Lifetime prevalence and age-of-onset distributions of DSM-IV disorders in the National Comorbidity Survey Replication. Arch Gen Psychiatry. 2005; 62:593–602. [PubMed: 15939837]

Lemogne C, Delaveau P, Freton M, Guionnet S, Fossati P. Medial prefrontal cortex and the self in major depression. J Affect Disord. 2012; 136:e1–e11. [PubMed: 21185083]

Leyton M, Paquette V, Gravel P, Rosa-Neto P, Weston F, Diksic M, Benkelfat C. alpha-[11C]Methyl-L-tryptophan trapping in the orbital and ventral medial prefrontal cortex of suicide attempters. Eur Neuropsychopharmacol. 2006; 16:220–3. [PubMed: 16269239]

Liu Q, Wong-Riley MT. Postnatal changes in tryptophan hydroxylase and serotonin transporter immunoreactivity in multiple brainstem nuclei of the rat: implications for a sensitive period. J Comp Neurol. 2010; 518:1082–97. [PubMed: 20127812]

Lu Y, Simpson KL, Weaver KJ, Lin RC. Coexpression of serotonin and nitric oxide in the raphe complex: cortical versus subcortical circuit. Anat Rec (Hoboken). 2010; 293:1954–65. [PubMed: 20734426]

McDevitt RA, Tiran-Cappello A, Shen H, Balderas I, Britt JP, Marino RA, Chung SL, Richie CT, Harvey BK, Bonci A. Serotonergic versus nonserotonergic dorsal raphe projection neurons: differential participation in reward circuitry. Cell Rep. 2014; 8:1857–69. [PubMed: 25242321]

Meloni EG, Reedy CL, Cohen BM, Carlezon WA Jr. Activation of raphe efferents to the medial prefrontal cortex by corticotropin-releasing factor: correlation with anxiety-like behavior. Biol Psychiatry. 2008; 63:832–9. [PubMed: 18061145]

Mintz EM, Scott TJ. Colocalization of serotonin and vesicular glutamate transporter 3-like immunoreactivity in the midbrain raphe of Syrian hamsters (Mesocricetus auratus). Neurosci Lett. 2006; 394:97–100. [PubMed: 16266785]

Muller JF, Mascagni F, McDonald AJ. Serotonin-immunoreactive axon terminals innervate pyramidal cells and interneurons in the rat basolateral amygdala. J Comp Neurol. 2007; 505:314–35. [PubMed: 17879281]

Muzerelle A, Scotto-Lomassese S, Bernard JF, Soiza-Reilly M, Gaspar P. Conditional anterograde tracing reveals distinct targeting of individual serotonin cell groups (B5-B9) to the forebrain and brainstem. Brain Struct Funct. 2014

Niederkofler V, Asher TE, Okaty BW, Rood BD, Narayan A, Hwa LS, Beck SG, Miczek KA, Dymecki SM. Identification of Serotonergic Neuronal Modules that Affect Aggressive Behavior. Cell Rep. 2016; 17:1934–1949. [PubMed: 27851959]

Okere CO, Waterhouse BD. Acute capsaicin injection increases nicotinamide adenine dinucleotide phosphate diaphorase staining independent of Fos activation in the rat dorsolateral periaqueductal gray. Neurosci Lett. 2006a; 404:288–93. [PubMed: 16835009]

Okere CO, Waterhouse BD. Acute restraint increases NADPH-diaphorase staining in distinct subregions of the rat dorsal raphe nucleus: implications for raphe serotonergic and nitrergic transmission. Brain Res. 2006b; 1119:174–81. [PubMed: 16989783]

Ongur D, Price JL. The organization of networks within the orbital and medial prefrontal cortex of rats, monkeys and humans. Cereb Cortex. 2000; 10:206–19. [PubMed: 10731217]

Pasquier DA, Villar MJ. Specific serotonergic projections to the lateral geniculate body from the lateral cell groups of the dorsal raphe nucleus. Brain Res. 1982; 249:142–6. [PubMed: 6291704]

Paxinos, G., Watson, C. The rat brain in stereotaxic coordinates. Academic Press; San Diego: 1997. Vol., ed.^eds

Phillips ML, Chase HW, Sheline YI, Etkin A, Almeida JR, Deckersbach T, Trivedi MH. Identifying predictors, moderators, and mediators of antidepressant response in major depressive disorder: neuroimaging approaches. Am J Psychiatry. 2015; 172:124–38. [PubMed: 25640931]

Piskuric NA, Vollmer C, Nurse CA. Confocal immunofluorescence study of rat aortic body chemoreceptors and associated neurons in situ and in vitro. J Comp Neurol. 2011; 519:856–73. [PubMed: 21280041]

Qi J, Zhang S, Wang HL, Wang H, de Jesus Aceves Buendia J, Hoffman AF, Lupica CR, Seal RP, Morales M. A glutamatergic reward input from the dorsal raphe to ventral tegmental area dopamine neurons. Nat Commun. 2014; 5:5390. [PubMed: 25388237]

Quirk GJ, Beer JS. Prefrontal involvement in the regulation of emotion: convergence of rat and human studies. Current opinion in neurobiology. 2006; 16:723–727. [PubMed: 17084617]

Richard JM, Berridge KC. Prefrontal cortex modulates desire and dread generated by nucleus accumbens glutamate disruption. Biol Psychiatry. 2013; 73:360–70. [PubMed: 22981656]

Rosin DL, Chang DA, Guyenet PG. Afferent and efferent connections of the rat retrotrapezoid nucleus. J Comp Neurol. 2006; 499:64–89. [PubMed: 16958085]

Sherman SM, Koch C. The control of retinogeniculate transmission in the mammalian lateral geniculate nucleus. Exp Brain Res. 1986; 63:1–20. [PubMed: 3015651]

Shikanai H, Yoshida T, Konno K, Yamasaki M, Izumi T, Ohmura Y, Watanabe M, Yoshioka M. Distinct neurochemical and functional properties of GAD67-containing 5-HT neurons in the rat dorsal raphe nucleus. J Neurosci. 2012a; 32:14415–26. [PubMed: 23055511]

Shikanai H, Yoshida T, Konno K, Yamasaki M, Izumi T, Ohmura Y, Watanabe M, Yoshioka M. Distinct neurochemical and functional properties of GAD67-containing 5-HT neurons in the rat dorsal raphe nucleus. The Journal of Neuroscience. 2012b; 32:14415–14426. [PubMed: 23055511]

Shutoh F, Ina A, Yoshida S, Konno J, Hisano S. Two distinct subtypes of serotonergic fibers classified by co-expression with vesicular glutamate transporter 3 in rat forebrain. Neurosci Lett. 2008; 432:132–6. [PubMed: 18222609]

Siegle GJ, Thompson W, Carter CS, Steinhauer SR, Thase ME. Increased amygdala and decreased dorsolateral prefrontal BOLD responses in unipolar depression: related and independent features. Biol Psychiatry. 2007; 61:198–209. [PubMed: 17027931]

Simpson KL, Waterhouse BD, Lin R. Differential expression of nitric oxide in serotonergic projection neurons: neurochemical identification of dorsal raphe inputs to rodent trigeminal somatosensory targets. Journal of Comparative Neurology. 2003; 466:495–512. [PubMed: 14566945]

Soghomonian JJ, Martin DL. Two isoforms of glutamate decarboxylase: why? Trends Pharmacol Sci. 1998; 19:500–5. [PubMed: 9871412]

Spiacci A Jr, Kanamaru F, Guimaraes FS, Oliveira RM. Nitric oxide-mediated anxiolytic-like and antidepressant-like effects in animal models of anxiety and depression. Pharmacol Biochem Behav. 2008; 88:247–55. [PubMed: 17915303]

Stamp JA, Semba K. Extent of colocalization of serotonin and GABA in the neurons of the rat raphe nuclei. Brain Res. 1995; 677:39–49. [PubMed: 7606468]

Stillman AA, Krsnik Z, Sun J, Rasin MR, State MW, Sestan N, Louvi A. Developmentally regulated and evolutionarily conserved expression of SLITRK1 in brain circuits implicated in Tourette syndrome. J Comp Neurol. 2009; 513:21–37. [PubMed: 19105198]

Sul JH, Kim H, Huh N, Lee D, Jung MW. Distinct roles of rodent orbitofrontal and medial prefrontal cortex in decision making. Neuron. 2010; 66:449–60. [PubMed: 20471357]

Suzuki Y, Kiyokage E, Sohn J, Hioki H, Toida K. Structural basis for serotonergic regulation of neural circuits in the mouse olfactory bulb. J Comp Neurol. 2015; 523:262–80. [PubMed: 25234191]

Van Bockstaele EJ, Biswas A, Pickel VM. Topography of serotonin neurons in the dorsal raphe nucleus that send axon collaterals to the rat prefrontal cortex and nucleus accumbens. Brain Res. 1993; 624:188–98. [PubMed: 8252391]

van Heeringen C, Audenaert K, Van Laere K, Dumont F, Slegers G, Mertens J, Dierckx RA. Prefrontal 5-HT2a receptor binding index, hopelessness and personality characteristics in attempted suicide. J Affect Disord. 2003; 74:149–58. [PubMed: 12706516]

Vasudeva RK, Lin RC, Simpson KL, Waterhouse BD. Functional organization of the dorsal raphe efferent system with special consideration of nitrergic cell groups. J Chem Neuroanat. 2011; 41:281–93. [PubMed: 21640185]

Vertes RP. A PHA-L analysis of ascending projections of the dorsal raphe nucleus in the rat. J Comp Neurol. 1991; 313:643–68. [PubMed: 1783685]

Vertes RP, Crane AM. Distribution, quantification, and morphological characteristics of serotonin-immunoreactive cells of the supralemniscal nucleus (B9) and pontomesencephalic reticular formation in the rat. J Comp Neurol. 1997; 378:411–24. [PubMed: 9034900]

Vertes RP, Linley SB, Hoover WB. Pattern of distribution of serotonergic fibers to the thalamus of the rat. Brain Struct Funct. 2010; 215:1–28. [PubMed: 20390296]

Villar MJ, Vitale ML, Hokfelt T, Verhofstad AA. Dorsal raphe serotoninergic branching neurons projecting both to the lateral geniculate body and superior colliculus: a combined retrograde tracing-immunohistochemical study in the rat. J Comp Neurol. 1988; 277:126–40. [PubMed: 3198794]

Vincent SR. Nitric oxide neurons and neurotransmission. Prog Neurobiol. 2010; 90:246–55. [PubMed: 19853011]

Voisin AN, Mnie-Filali O, Giguere N, Fortin GM, Vigneault E, El Mestikawy S, Descarries L, Trudeau LE. Axonal Segregation and Role of the Vesicular Glutamate Transporter VGLUT3 in Serotonin Neurons. Front Neuroanat. 2016; 10:39. [PubMed: 27147980]

Walther DJ, Peter J-U, Bashammakh S, Hörtnagl H, Voits M, Fink H, Bader M. Synthesis of Serotonin by a Second Tryptophan Hydroxylase Isoform. Science. 2003; 299:76–76. [PubMed: 12511643]

Waterhouse BD, Border B, Wahl L, Mihailoff GA. Topographic organization of rat locus coeruleus and dorsal raphe nuclei: distribution of cells projecting to visual system structures. J Comp Neurol. 1993; 336:345–61. [PubMed: 8263226]

Wotherspoon G, Albert M, Rattray M, Priestley JV. Serotonin and NADPH-diaphorase in the dorsal raphe nucleus of the adult rat. Neurosci Lett. 1994; 173:31–6. [PubMed: 7523999]

Yamamoto K, Takei H, Koyanagi Y, Koshikawa N, Kobayashi M. Presynaptic cell type-dependent regulation of GABAergic synaptic transmission by nitric oxide in rat insular cortex. Neuroscience. 2015; 284:65–77. [PubMed: 25286388]

Highlights

- Nearly all labeled 5-HT cells expressed VGLUT3 regardless of their efferent target
- Very few labeled 5-HT neurons expressed GAD67 and nearly all targeted the LGN
- nNOS was detected in a greater percentage of 5-HT cells projecting to mPFC vs. LGN

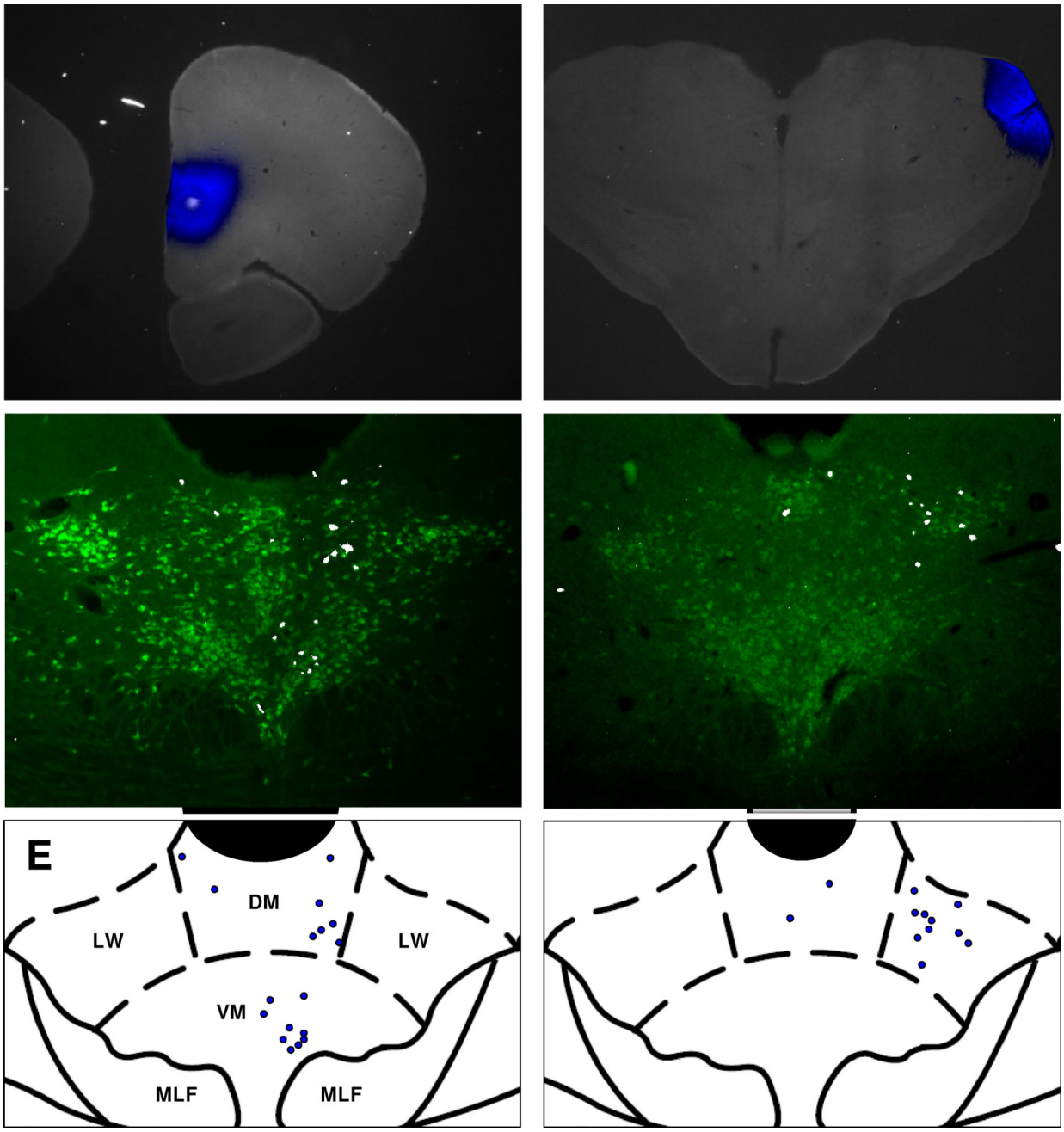

Figure 1. Anatomical distribution of labeled neurons within the DR

A–B, representative photomicrographs of FG injections (blue) into the mPFC (**A**) or LGN (**B**). **C-D**, coronal sections through the brainstem showing representative distributions of FG-labeled neurons (white) that project to mPFC (**C**) or LGN (**D**). Serotoninergic neurons are shown in green. **E-F**, Coronal atlas images showing the borders and sub-divisions of the DR near its widest point (bregma −8 mm). Blue circles indicate the locations of FG-labeled neurons from **C** and **D**. Aq = cerebral aqueduct. DM = dorsomedial, VM = ventromedial, LW = lateral wing, MLF = medial longitudinal fasciculus. In **1C** and **1D**, FG fluorescence was pseudocolored to white for better visibility at small size; FG fluorescence was

pseudocolored to blue in all other images that contain FG signal. Stereotaxic atlas images adapted from Paxinos and Watson, 1997.

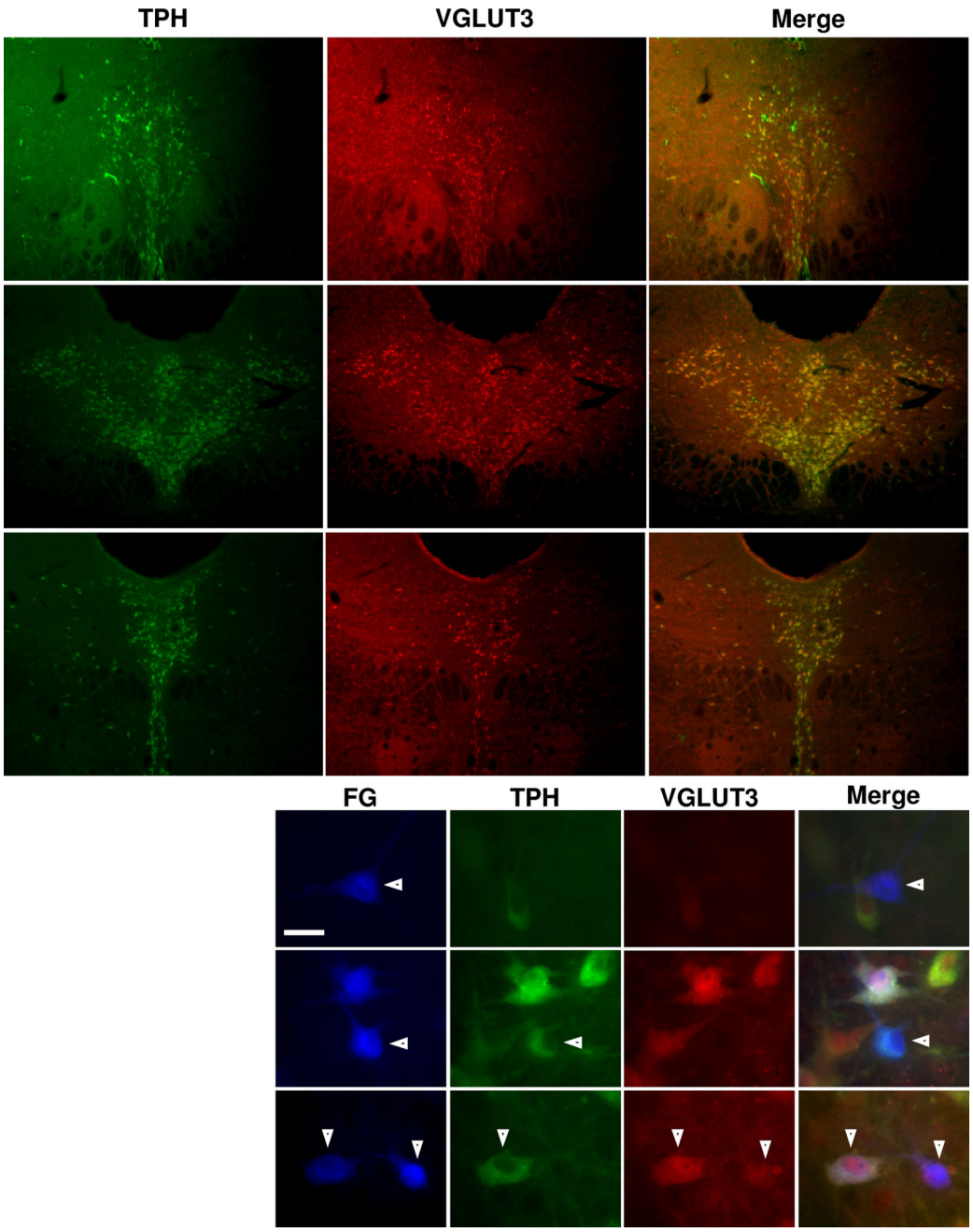

Figure 2. TPH and VGLUT3 expression and co-localization in the DR

Each row represents photomicrographs containing the same field of view taken through different fluorescence filters. The columns represent photomicrographs taken through the same fluorescence filter; the filters are specific for the neurochemical marker listed above each column. The Merge column is a composite overlay of the preceding images from each row. **A-C**, Low power photomicrographs showing the expression of TPH (green) and VGLUT3 (red) in coronal sections of brainstem tissue at three different levels along the rostrocaudal extent of the DR. **A1-3**, rostral DR (7.0 mm caudal to bregma). **B1-3**, intermediate DR (7.8 mm caudal to bregma). **C1-3**, caudal DR (8.1 mm caudal to bregma).

D, High power photomicrographs showing the immunoreactivity of FG-labeled neurons within the DR. Arrowheads and roman numerals indicate representative neurons with different immunoreactive profiles. Neuron negative for both TPH and VGLUT3 (**i**), neuron positive for TPH and negative for VGLUT3 (**ii**), neuron positive for both TPH and VGLUT3 (**iii**), neuron negative for TPH and positive for VGLUT3 (**iv**). Scale bar = 20 μm.

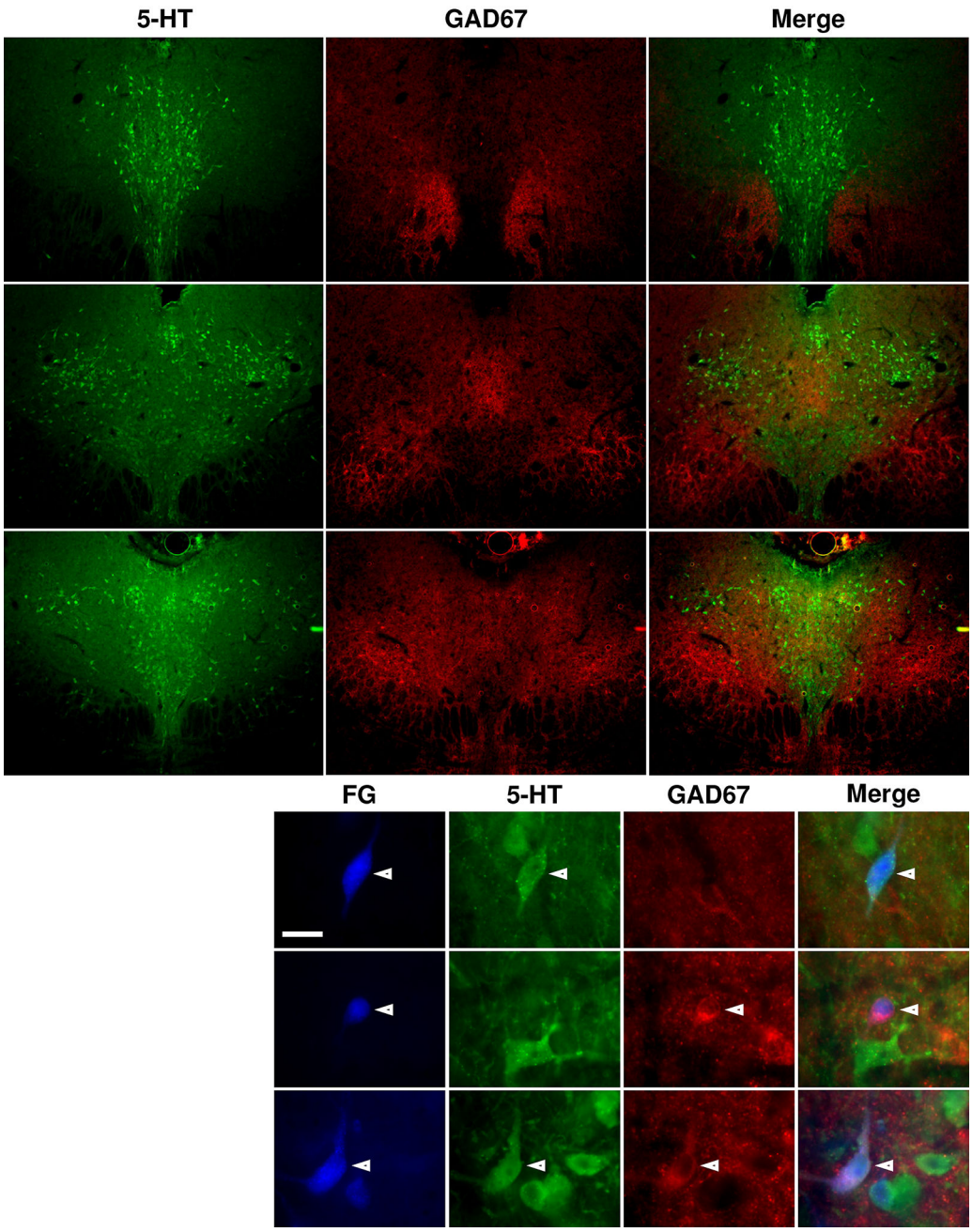

Figure 3. 5-HT and GAD67 expression and co-localization in the DR

A–C, Low power photomicrographs showing the expression of 5-HT (green) and GAD67 (red) in coronal sections of brainstem tissue at three different levels along the rostrocaudal extent of the DR. Labeling for rows and columns follow the same conventions as in Fig. 2. **A1-3**, rostral DR (7.1 mm caudal to bregma). **B1-3**, intermediate DR (7.6 mm caudal to bregma). **C1-3**, caudal DR (8.0 mm caudal to bregma). **D**, High power photomicrographs showing the immunoreactivity of FG-labeled neurons within the DR. Arrowheads and roman numerals indicate representative neurons with different immunoreactive profiles. Neuron

positive for 5-HT and negative for GAD67 (**i**), neuron negative for 5-HT and positive for GAD67 (**ii**), neuron positive for 5-HT and GAD67 (**iii**). Scale bar = 20 μm.

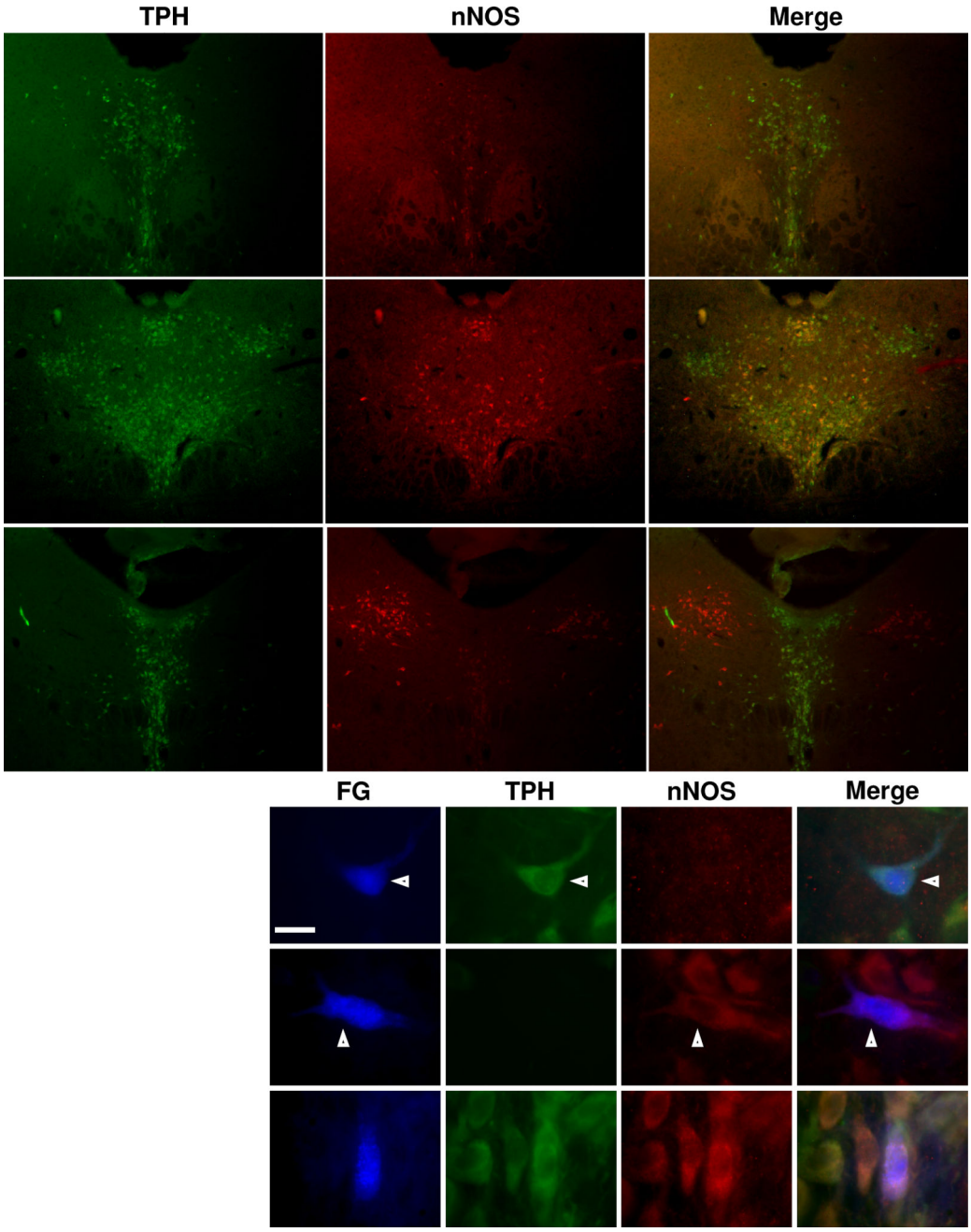

Figure 4. TPH and nNOS expression and co-localization in the DR

A–, Low power photomicrographs showing the expression of TPH (green) and nNOS (red) in coronal sections of brainstem tissue at three different levels along the rostrocaudal extent of the Labeling for rows and columns follow the same conventions as in Fig. 2. DR. **A1-3**, rostral DR (7.1 mm caudal to bregma). **B1-3**, intermediate DR (7.6 mm caudal to bregma). **C1-3**, caudal DR (8.0 mm caudal to bregma). **D**, High power photomicrographs showing the immunoreactivity of FG-labeled neurons within the DR. Arrowheads and roman numerals indicate representative neurons with different immunoreactive profiles. Neuron positive for

TPH and negative for nNOS (**i**), neuron negative TPH and positive for nNOS (**ii**), neuron positive for TPH and nNOS (**iii**). Scale bar = 20 μm.

Table 1

Immunoreactivity counts of mPFC-projecting DR neurons stained for TPH and VGLUT3

Case	FG-only	VGLUT3-only	TPH-only	TPH and VGLUT3	Total
1	2	8	2	79	91
2	5	11	1	110	127
3	5	13	4	95	117
4	9	20	3	145	177
5	1	14	4	147	166
6	2	9	0	122	133
Total	**24**	**75**	**14**	**698**	**811**
Total %	**3**	**9**	**2**	**86**	**100**

Table 2

Immunoreactivity counts of LGN-projecting DR neurons stained for TPH and VGLUT3

Case	FG-only	VGLUT3-only	TPH-only	TPH and VGLUT3	Total
1	0	4	0	108	112
2	1	1	0	87	89
3	8	5	5	205	223
4	7	6	2	100	115
5	2	7	0	134	143
6	6	4	4	88	102
Total	**24**	**27**	**11**	**722**	**784**
Total %	**3**	**4**	**1**	**92**	**100**

Table 3

Immunoreactivity counts of mPFC-projecting DR neurons stained for 5-HT and GAD67

Case	FG-only	GAD67-only	5-HT-only	5-HT + GAD67	Total
1	14	0	130	0	144
2	11	0	143	0	154
3	5	0	103	0	108
4	14	0	157	0	171
5	11	0	111	0	122
6	7	0	87	1	95
Total	**62**	**0**	**731**	**1**	**794**
Total %	**7.8**	**0**	**92.1**	**0.1**	**100**

Table 4

Immunoreactivity counts of LGN-projecting DR neurons stained for 5-HT and GAD67

Case	FG-only	GAD67-only	5-HT-only	5-HT and GAD67	Total
1	3	0	98	3	104
2	1	0	68	0	69
3	6	0	97	1	104
4	4	0	124	1	129
5	9	1	145	1	156
6	3	0	100	1	104
Total	**26**	**1**	**632**	**7**	**666**
Total %	**3.9**	**0.1**	**94.9**	**1.1**	**100**

Table 5

Immunoreactivity counts of mPFC-projecting DR neurons stained for TPH and nNOS

Case	FG-only	nNOS-only	TPH-only	TPH and nNOS	Total
1	7	0	44	45	96
2	12	0	38	54	104
3	13	3	40	52	108
4	10	1	41	69	121
5	10	0	36	75	121
6	3	0	32	48	83
Total	**55**	**4**	**231**	**343**	**633**
Total %	**9**	**1**	**36**	**54**	**100**

Table 6

Immunoreactivity counts of LGN-projecting DR neurons stained for TPH and nNOS

Case	FG-only	nNOS-only	TPH-only	TPH and nNOS	Total
1	0	1	80	33	114
2	1	0	57	23	81
3	2	9	79	23	113
4	3	4	106	19	132
5	1	5	110	20	136
6	2	2	65	22	91
Total	**9**	**21**	**497**	**140**	**667**
Total %	**1**	**3**	**75**	**21**	**100**

Table 7

Summary of antibodies and staining combinations

Neurochemical marker	Primary antibodies	Secondary antibodies
TPH + VGLUT3	Mouse anti-TPH (1:500)	Goat anti-mouse Alexa Fluor 488 (1:200)
	Rabbit anti-VGLUT3 (1:200)	Goat anti-rabbit Alexa Fluor 555 (1:500)
5-HT + GAD67	Rabbit anti-5-HT (1:2000)	Goat anti-rabbit Alexa Fluor 555 (1:500)
	Mouse anti-GAD67 (1:500)	Goat anti-mouse Alexa Fluor 488 (1:200)
TPH + nNOS	Mouse anti-TPH (1:500)	Goat anti-mouse Alexa Fluor 488 (1:200)
	Rabbit anti-nNOS (1:1000)	Goat anti-rabbit Alexa Fluor 555 (1:250)